Environmental Science and Pollution Research (2019) 26:3065–3074
https://doi.org/10.1007/s11356-018-3815-z

RESEARCH ARTICLE

Study on the influence of surface potential on the nitrate adsorption capacity of metal modified biochar

Li Long[1] · Yingwen Xue[1] · Xiaolan Hu[1] · Ying Zhu[1]

Received: 1 August 2018 / Accepted: 20 November 2018 / Published online: 1 December 2018
© Springer-Verlag GmbH Germany, part of Springer Nature 2018

Abstract

Carbon materials, as effective adsorbents to numerous aqueous cationic contaminants, have been hardly applied to remove anions in wastewater. In this work, different modifying agents were used to modify corncob biochars (CC) and the surface potentials of these modified biochars were determined. Based on the findings, modification principle was determined to reveal the relationship between surface potentials of the biochars and their nitrate adsorption capacities. The surface potential was dominated by the metal cations and multivalent cations led to even positive zeta potential. The formation of metal oxide not only led to the augment in surface area but also increase the surface charge. $FeCl_3$-modified biochar (Fe-CC) with the highest positive surface charge was utilized to remove anions (nitrate) from aqueous solutions. Characterization results confirm that Fe_2O_3 structure were successfully formed on biochar surface. This led to the formation of iron nitrate hydrate ($Fe(NO_3)_3{\cdot}9H_2O$), which enabled higher nitrate adsorption performance than that of pristine biochar. Batch experiments showed that nitrate adsorption on the Fe-CC was stable and almost independent of experimental pH and temperature. Based on the Langmuir model results, the maximum nitrate adsorption capacity of Fe-CC was 32.33 mg/g. Coexisting anions had negative influence on the adsorption performance. Findings of this work suggest that the modified biochar can be used in wastewater treatment to remove anions such as nitrate.

Keywords Metal modified biochar · Surface charge · Zeta potential · Modification principle · Adsorption mechanism

Introduction

With the rapid development of modern agriculture and the acceleration of urban modernization, nitrate pollution has become a serious problem. Therefore, nitrate pollution in underground and surface water has attracted much research attention around the world. Due to its high water solubility, nitrate has been found in all kinds of water bodies, which can pose a serious threat to environment and human health. In addition to eutrophication, the increase of nitrate concentration can also cause human health problems such as (1) it can cause methemoglobinemia to babies, commonly known as "Blue baby syndrome"; (2) it is easy to form nitrosamine compounds to induce cancer; and (3) it can lead to diminished intelligence for reducing oxygen supply in body cells. Therefore, it has been a hot subject for researchers to take an economical-efficient and environmental friendly way to treat nitrate pollution.

Recently, biological treatment and physical and chemical removal methods have been applied to treat nitrate pollution (Du et al. 2017; Hu et al. 2018a; Villegas-Guzman et al. 2017). Adsorption has attracted universal attention for its unique characterizations, such as considerable removal efficiency and environmental friendly process. Among numerous adsorbents, carbon materials have been prevailing adsorbents for removing contaminants. Carbon adsorbents including graphene (Wang et al. 2017), carbon nanotubes (Kang et al. 2018), activated carbon (Liu et al. 2016a), and biochar (Hu et al. 2018a) are widely applied to remove aqueous contaminants.

To further improve their adsorption capacities, carbon adsorbents are often modified. To data, there have been numerous modification methods for carbon materials. Hummers, Brodie, and Staudenmaier methods are three graphene modification methods (Sofer et al. 2015). These synthesis ways lead to a grapheme oxide product with varying C/O ratios and oxygen functionalities on graphene basal planes and edge

Responsible editor: Tito Roberto Cadaval Jr

✉ Yingwen Xue
ywxue@whu.edu.cn

[1] School of Civil Engineering, Wuhan University, Wuhan, China

sites. Therefore, these modification methods can make significant influences on the adsorption capacities of graphene. Oxidation, alkali activation, and modification with other components are common chemical modification methods to improve nanotubes' properties. In these processes, various functional groups can be generated or introduced onto nanotube surfaces (at tips and sidewalls) for the removal of environmental contaminants (Sarkar et al. 2018). In the modification of activated carbon, thermal contraction (Qiu et al. 2017) and vapor activation (Lu et al. 2016) are aimed to increase the surface area or adjust pore structure and its distribution. Due to the effects of functional groups and chemical constitution on adsorption, chemical modifications are mainly used to change the surface acidity and basicity, introduce or remove functional groups (Long et al. 2017).

Biochar, an emerging carbon adsorbent, possesses a great adsorption capacity to many contaminants (Liu et al. 2016b; Yao et al. 2011; Yu et al. 2016). The modifications of biochar are divided into pre- and post-modification. These make the biochar physical structure and chemical component changed, which is helpful for adsorption process. To date, previous articles indicated that most of the unmodified and modified biochars possessed negative charge on the surface (Yao et al. 2011). Therefore, it has been demonstrated that biochar is a wonderful adsorbent for cationic pollutants, especially metal ions (Xiao et al. 2017) because of its negative charged surface. Most modifications have been mainly aimed to increase the negative charge so that the adsorption capacities can be improved. Ding produced engineer biochar from hickory wood and then further modified with NaOH (Ding et al. 2016). After modification, the modified biochar exhibits much larger metal adsorption capacities than the pristine biochar. Creamer used metal ions to treat feedstocks to produce metal oxyhydroxide-biochar composites and these modified biochars effectively capture CO_2 (Creamer et al. 2016).

There are only few studies on anions adsorption on biochar. According to previous articles, the mechanisms of biochar to remove anions can be divided into three types: precipitation (chemical reaction occurrence), electrostatic attraction (surface charge domination), and physical adsorption (high surface area determination) (Jung et al. 2017; Wang et al. 2016; Yao et al. 2012; Zhang et al. 2016). The challenge of nitrate removal is due to the high soluble ability of nitrate. For other common anions like phosphate, the immobilization could be easy to achieve by the chemical reactions of some metal ions. But for nitrate, little chemical precipitation methods could be used to immobilize nitrate.

Previous studies have investigated the impact of surface charge of biochars is sorption of anions. Wan et al. (2017) examined phosphate adsorption of bamboo biochar functionalized with varying amount of Mg–Al layered double hydroxides. Xue et al. (2016) used Mg–Fe layered double hydroxide biochar to remove nitrate and the maximum adsorption capacity was 24.8 mg/g. Zhang et al. (2013) prepared Mg–Al layered double hydroxides biochar and this biochar was an effective sorbent for the removal of phosphate. Wang et al. (2016) used hydrochloric acid as post modifying agent to modify biochar to enhance nitrate removal in constructed wetland, whose adsorption capacity was 14.67 mg/g. They discovered zeta potentials of the biochar increased from − 12.23 to + 5.46 mV after modification. It had been reported in some articles that positive zeta potential led to high anion adsorption capacity. Zhang et al. (2016) used Fe^{2+}/Fe^{3+} to modify hyacinth biomass and then prepared modified biochar with low positive-charged surface to remove arsenate and obtained a capacity of 7.4 mg/g, which is attributed to the unique iron substances formed by novel modification. Jung et al. (2017) prepared a novel magnesium ferrite biochar and used it to remove phosphate. The pH_{pzc} of the modified biochar is 8.52. Nevertheless, these papers have neither discussed the possible modifying principle to increasing the surface charge, nor determined the relationship between surface charge and adsorption capacity. Therefore, the goal of this work is aimed to clarify the modification principle to further increase the positive surface charge on biochar and then use the modified biochar to remove anions, especially nitrate.

Based on the conclusions of previous researches, the specific objectives of this work are to (1) study the effect of different modifying agents on biochar's ability to remove nitrate; (2) analyze the relationship between surface charge and adsorption capacity and thus reveal the modification principle; and (3) clarify the adsorption mechanism of biochar to anions.

Materials and methods

Materials

All the chemical reagents of analytical grades in this experiment were acquired from Sinopharm Chemical Reagent Co., Ltd, and the corncob was from a local farm (Wuhan, China). Deionized water was used to prepare chemical solutions.

Biochar production

The feedstock (corncob) was rinsed and then dried in a drying oven at the temperature of 80 °C (Liu et al. 2016b). To prepare pristine biochar, the corncob sample was pyrolyzed in quartz tubes at the temperature of 600 °C with N_2 flowing for 2 h. The black remainder (bulk biochar) in the quartz tube was ground and then sieved to a uniform size of 0.9~1.2 mm. Finally, the ground biochar was rinsed by DI water, dried, and stored for adsorption experiments (Gao et al. 2015; Hu et al. 2018b). To prepare modified biochars, eight samples of corncob were respectively dipped in 1 mol/L modifying agent solutions (HCl, NaCl, KCl, $MgCl_2$, $ZnCl_2$, $AlCl_3$, $FeCl_3$,

$MgCl_2$ with HCl) for 24 h with the impregnation ratio of 3 g:1 g. The modified feedstocks were treated the same way as the pristine ones to prepare the modified biochars. Finally, these nine biochars were labeled as CC, H-CC, Na-CC, K-CC, Mg-CC, Al-CC, Fe-CC and H + Mg-CC, respectively.

Characterization

The surface charge was obtained using a zeta potential analyzer (Zetasizer Nano ZS, Malvern, UK). The element analysis was measured by element analyzer (Vario EL III, Elementar, German) and the specific surface areas were measured by a surface area analyzer (TriStar II 3020, Micromeritics, USA). The surface morphology was obtained using a scanning electron microscopy (SEM, JEM-6700F, Hitachi Limited, Japan). Fourier transform infrared spectroscopy (FTIR, NICOLET 5700, Thermo Electron Corporation, USA) was used to determine the surface functional groups on the biochars. The crystalline minerals if the biochar samples were investigated by a computer controlled X-ray diffractometer (XRD, PANalytical, X'Pert Pro, Netherlands).

Static adsorption test

0.1 g biochar was added into 50 ml NO_3^- solution (100 ppm). After being shaken in the mechanical shaker (120 r/min) at the temperature of 30 °C for 24 h, the mixture was filtered through 0.22-μm membrane filter to achieve solid-liquid separation. Concentrations of NO_3–N were determined by the ion chromatograph (882 Compact IC plus; Metrohm, Herisau, Switzerland).

The adsorption amount q (mg/g) and adsorption removal rate R (%) of nitrate were calculated by formula (1) and formula (2) based on the difference between the initial and final aqueous concentrations (Tanboonchuy et al. 2011):

$$q = \frac{(C_0 - C_e)V}{m} \quad (1)$$

$$R = \frac{C_0 - C_e}{C_0} \times 100 \quad (2)$$

where C_0 and C_e are the initial and equilibrium concentration of nitrate solution respectively (mg/L); m is the weight of biochar adsorbent (g); and V is the volume of solution (ml).

Effect of pH, reaction temperature, and coexisting anions

The influence of three environmental factors on nitrate removal was studied (Table 1). The initial nitrate concentrations were all 100 ppm and the shaking speeds were all 120 r/min with the reaction time of 24 h. Various pH, temperature, and coexisting anions were evaluated. pH was adjusted by NaOH or HCl (0.01 mmol/L, 1 mmol/L, and 100 mmol/L) solutions and measured by a pH meter (FE20, Mettler Toledo (Shanghai) Co., Ltd.).

Mathematical models

Sorption kinetics of NO_3^- (50 ppm) onto the biochar were evaluated by the similar process as static test. What was different was that the adsorption time changed to 0.5, 1, 2, 5, 10, 15, 20, 24, 48 h. The pseudo-first-order, pseudo-second-order, and Elovich models were used to simulate the sorption kinetics data and their governing equations can be written as (Eeshwarasinghe et al. 2018):

$$\text{Pseudo-first-order} : q_t = q_e\left(1 - e^{-k_1 t}\right) \quad (3)$$

$$\text{Pseudo-second-order} : q_t = \frac{k_2 q_e^2 t}{1 + k_2 q_e^2 t} \quad (4)$$

$$\text{Elovich} : q_t = \frac{1}{\beta}\ln(\alpha\beta t + 1) \quad (5)$$

where q_t and q_e are the amount of sorbate removed at time t and at equilibrium, respectively (mg/g); k_1 and k_2 are the first-order and second-order sorption rate constants (h^{-1}), respectively; α is the initial sorption rate (mg/g) and β is the desorption constant (g/mg), the Elovich model is an empirical fitting equation.

Adsorption isotherms of NO_3–N onto the biochar were evaluated by a process similar to the kinetic test. The different was that the initial NO_3–N concentration was changed to 50, 100, 250, 400, 600, 750, 900, 1000, and 1500 ppm. The sorption isotherms were simulated by the Langmuir and Freundlich models, whose governing equations can be written as (Tytak et al. 2015):

$$\text{Langmuir} : q_e = \frac{K S_{max} C_e}{1 + K C_e} \quad (6)$$

$$\text{Freundlich} : q_e = K_f C_e^{1/n} \quad (7)$$

where K and K_f are the Langmuir bonding term correlated with interaction energies (L/mg) and the Freundlich affinity coefficient ((mg/g) $(1/mg)^{1/n}$), respectively; S_{max} is the Langmuir maximum capacity (mg/g), C_e is the equilibrium solution concentration (mg/L) of the sorbate, and n is the Freundlich linearity constant. The Langmuir model assumes that monolayer adsorption onto a homogeneous surface without interactions between the adsorbed molecules. The Freundlich model commonly used for heterogeneous surface as an empirical equation.

Table 1 Experiment of influencing factors

Influencing factors	Method	Value
Coexisting anions	Preparing Cl^-, CO_3^{2-}, PO_4^{3-} solutions	Every solute concentration was 100 mg/L
pH	Using pH meter	3, 5, 7, 9, and 11
Reaction temperature	Adjusting mechanical shaker temperature	15 °C, 25 °C, 30 °C, 35 °C, and 45 °C

Results and discussion

Comparison of biochars

Previous studies have demonstrated a positive correlation between the adsorbent surface charge and its zeta potential (Calero et al. n.d.; Patwardhan et al. 2012). In this work, the surface charge of modified biochars was determined by measuring zeta potential at neutral pH. These modified biochars could be obviously divided into three groups (Fig. 1). K-CC and Na-CC were both around − 50 mV, Zn-CC and Mg-CC were both around − 10 mV, and Al-CC and Fe-CC were around + 35 mV. This observation indicates that the zeta potential of modified biochar was dominated by modifying agents. The different modifying agents led to huge differences in zeta potential, but not all metal modification increased the zeta potential. Compared with pristine biochar (− 23.73 mV), the higher valence of modifying metal caused more increase of zeta potential, even making it become positive (+ 42.67 mV of Fe-CC and + 29.00 mV of Al-CC). This implies that the surface charge of modified biochars were most attributed to the metal valence rather than the metal group. Considering some solutions of modifying agents were acidic, the influence of $MgCl_2$ agents with HCl was assessed. There was a slight increase of zeta potentials after acid treatment. This indicates that at acidic solution, the modification efficient was improved to some extent. Furthermore, there were distinct differences of adsorption capacity among different modified biochars. The adsorption capacities of Zn-CC, Al-CC, and Fe-CC were all beyond 9.5 mg/g; while those of Na-CC, K-CC, and Mg-CC were limited (below 2 mg/g). It is indicated in Fig. 2 that with the increase of zeta potential, the adsorption capacity increased. Notably, there was an abrupt jump around − 9 mV. This implies that the zeta potential played a vital role in adsorption until it reached around − 9 mV. As the zeta potential rose above − 9 mV, the electrostatic repulsion resulted from negative surface charge was not dominative in the adsorption and other factors caused the significant increase.

Compared with pristine biochar, the C content of all modified biochars decreased while H and N contents were stable (Table 2). After modification, the relevant metal content significant increased, making the zeta potential increase in some sense. The slight difference of element contents between H + Mg-CC and Mg-CC indicated that acidic condition was in favor of the formation of metal substance onto modified biochar. Among these modified biochars, higher valence metal elements seemed to introduce more corresponding metal element content onto the modified biochars. This observation is consistent with the analysis in zeta potential that the higher valence of modifying metal led to higher Zeta potential. The Fe content in Fe-CC reached 8.795%. This constituted a basic

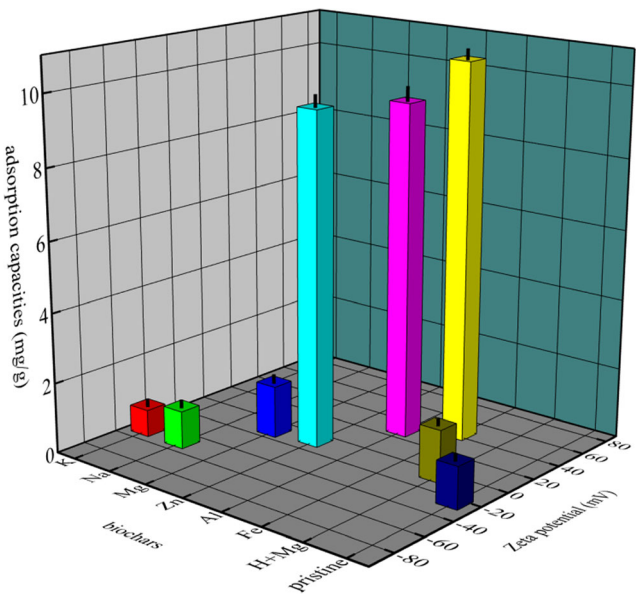

Fig. 1 The zeta potentials and nitrate adsorption capacities of different modified biochars

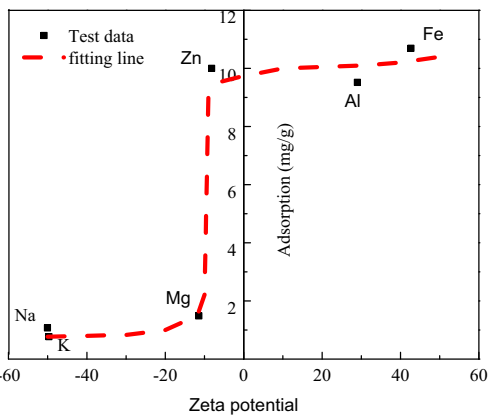

Fig. 2 The comparison of different modified biochar with zeta potential

Table 2 The element composition of different biochars

Adsorbent	Element content (mg/g)								
	C	N	H	Na	K	Mg	Zn	Al	Fe
CC	85.14	0.39	1.76	0.1975	1.0325	0.0775	0.02225	0.01175	0.135
Na-CC	83.24	0.36	1.69	2.0075					
K-CC	84.34	0.38	1.90		1.985				
Mg-CC	79.67	0.34	1.80			5.465			
Zn-CC	73.59	0.50	1.75				5.9		
Al-CC	61.37	0.36	1.22					3.335	
Fe-CC	75.52	0.43	1.80						8.7975
H + Mg-CC	74.96	0.35	1.59			6.0975			

foundation to the highest surface charge in the analysis of zeta potential (Yao et al. 2011), making high anion adsorption capacity feasible.

The specific surface area analysis showed that modification had huge influence on surface morphology of the biochars. Compared with CC, some modified biochars (Mg-CC, Zn-CC, Al-CC, Fe-CC) had higher surface area, while Na-CC and K-CC had lower. This difference is partly similar to the observations in surface charge analysis that Mg-CC, Zn-CC, Al-CC, and Fe-CC possessed higher zeta potential than that of pristine CC, while those of Na-CC and K-CC were lower (Fig. 2).

XRD testing was applied to determine the crystallinity and type of metal component in the samples. Compared with pristine biochar, there were some new-formed metal dioxide structures on the modified biochars (Fig. 3). These metal structures (Fe_2O_3, $MgAl_2O_4$, MgO, ZnO) were in favor of the increase of zeta potentials and the surface area in some extent (Long et al. 2017; Zhang et al. 2012). The ZnO formed on Zn-CC and the MgO formed on Mg-CC just increased the zeta potentials from −20 to −9 mV. $MgAl_2O_4$ is a double oxide structure and this special metal structure might lead to the positive surface charge of Al-CC (Cosimo et al. 1998; Wan et al. 2017). This positive surface charge (+29 mV) play a role in adsorption of nitrate. Fe_2O_3 significantly increased the surface charge to +43 mV and there was a peak of iron nitrate hydrate ($Fe(NO_3)_3{\cdot}9H_2O$) in Fe-CC after nitrate adsorption, which might explain the highest adsorption capacity of Fe-CC.

The FTIR spectra (Fig. 4) show that biochars possessed abundant functional groups. All modified biochars

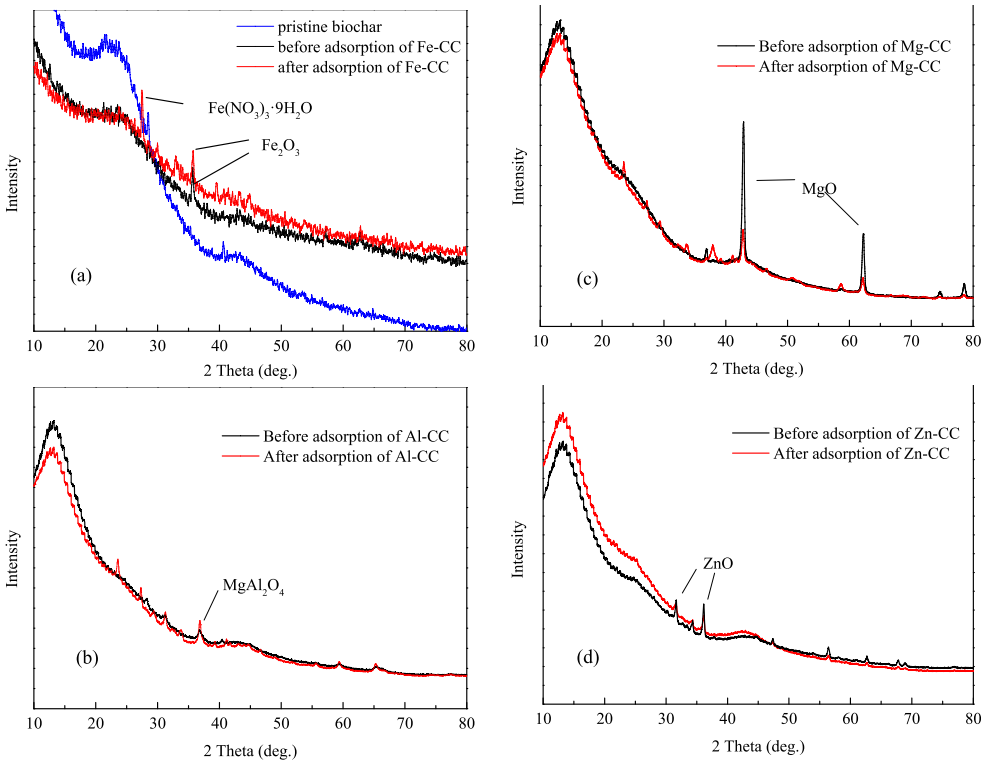

Fig. 3 XRD analysis of biochars: **a** CC and Fe-CC, **b** Al-CC, **c** Mg-CC, and **d** Zn-CC

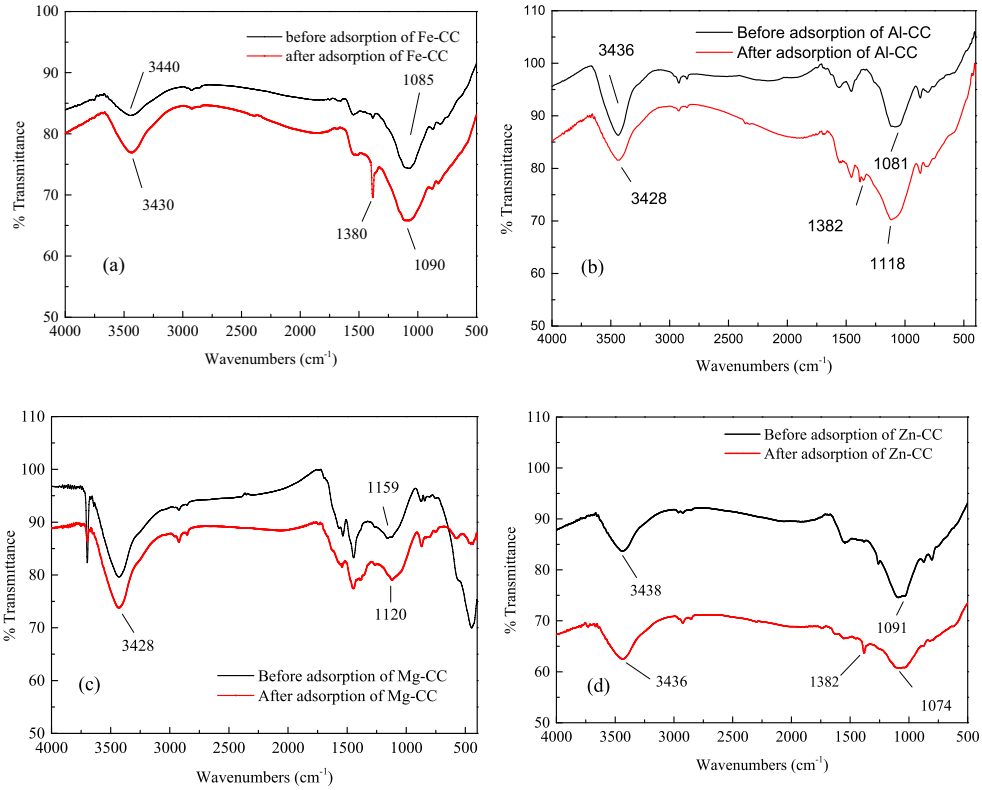

Fig. 4 FTIR spectrum of biochars: **a** CC and Fe-CC, **b** Al-CC, **c** Mg-CC, and **d** Zn-CC

possessed the O–H (around 3435) stretching and the C–O stretch (around 1080) (Xue et al. 2012). After adsorption, the peak observed at 1380 cm^{-1} in Fig. 4a, b, d designates nitrate (Choe et al. 2010; Sembiring et al. 2014), indicating Fe-CC and Al-CC with positive surface charge were much easier to attract nitrate anions. Taking the similarities of Zn-CC and Mg-CC in the analyses of zeta potential, BET and XRD into consideration, the metal Zn probably formed coordination compound (De et al. 2014), which is indirectly confirmed in Fig. 4d. The iron nitrate hydrate ($Fe(NO_3)_3{\cdot}9H_2O$) generated after the adsorption of Fe-CC is a coordination compound. By comparing the effect of these modified biochar, the best biochar (Fe-CC) was selected as adsorbent to remove nitrate.

Modifying principle

These observations indicate that modification played a crucial part in preparing modified biochars for nitrate removal. Metal-modifying agents are high likely to fix metal ion on the biochars by forming metal oxide and this makes a huge influence

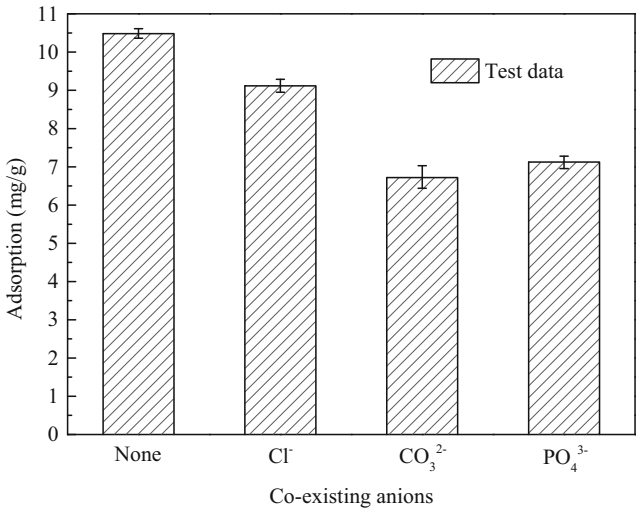

Fig. 5 Effect of coexisting anions on the adsorption of Fe-CC

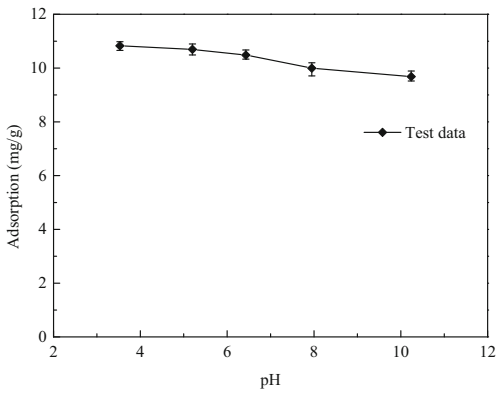

Fig. 6 Effect of pH on the adsorption of Fe-CC

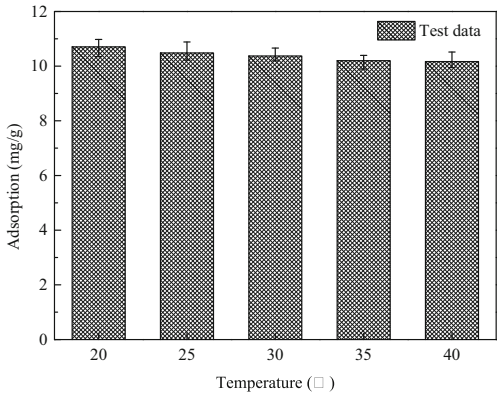

Fig. 7 Effect of temperature on the adsorption of Fe-CC

on properties of modified biochars. Metal oxide structure is in favor of the increase of specific surface area and zeta potential. Metal valence plays a vital role and higher metal valence meant higher surface area and higher zeta potential. High-specific surface area is beneficial for surface adsorption. Meantime higher zeta potential means higher surface charge, which is helpful for electrostatic attraction. In addition, some metal content which possessed multilayer electrons possibly formed special component such as coordination compound in the adsorption process, which made corresponding modified biochar have higher adsorption capacities. Therefore, metal possessing multilayer electrons with higher valence was a better modifying agent for the adsorption to anions.

Effect of coexisting anions, pH, and adsorption temperature

It is common that nitrate is coexisting with Cl^-, CO_3^{2-}, and PO_4^{3-} in the wastewater. These three coexisting anions had different valences. All anions made negative influences on nitrate adsorption on the biochars (Fig. 5). With the increase in negative charge of anions, the surface charge decreased and less adsorption sites were available to nitrate so the adsorption capacity declined. This indicated that adsorption process of Fe-CC was influenced by electrostatic attraction (Wang et al. 2015).

The effect of solution pH on the removal of nitrate was studied by varying the initial pH between 3 and 11 (Fig. 6). The increase in pH had little influence on the adsorption and the adsorption capacity of nitrate onto Fe-CC was steadily with values all beyond 9.5 mg/g. Although pH increased, the Fe-CC possessed several properties, such as huge surface area, high positive surface charge, and unique multilayer electrons, to maintain adsorption capacity. This was vital for Fe-CC to be used to treat real wastewater whose pH varies from acidity to alkalinity.

Changes in reaction temperature only slightly affected the adsorption of nitrate onto Fe-CC (Fig. 7). The capacity only decreased slightly with the increase of temperature from 20 to 40 °C. This endurance of temperature changes made Fe-CC suitable in real water treatment.

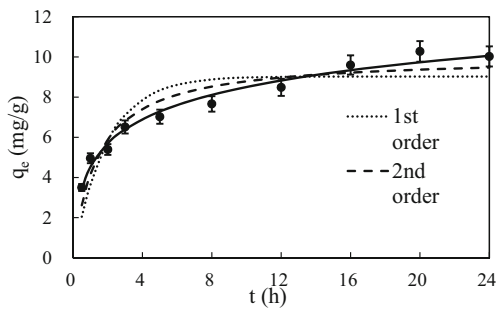

Fig. 8 Kinetics of nitrate adsorption onto Fe-CC

Table 3 Kinetic parameters of nitrate adsorption by Fe-CC

Kinetics	Parameters				
	q_e (mg/g)	k (h-1)	α (g/mg)	β (mg/g)	R^2
Pseudo-first-order	9.027	0.516	–	–	0.773
Pseudo-second-order	10.030	0.071	–	–	0.902
Elovich	–	–	20.858	0.561	0.978

Adsorption kinetics and isotherms

The pseudo-first-order, pseudo-second-order, and Elovich models were applied to describe the kinetics of nitrate adsorption (Fig. 8). The model results of kinetic data are presented in Table 3. High correlation coefficient value ($R^2 = 0.978$) suggest good agreement between the experimental data and fitting curve of Elovich, confirming that the adsorption of nitrate onto Fe-CC followed the Elovich model best. While the correlation coefficients of the pseudo-first- and second-order were only 0.773 and 0.902 respectively. Similar results about anions adsorption were obtained in the removal of trichloroacetic acid on modified biochar derived from crayfish shell (Long et al. 2017).

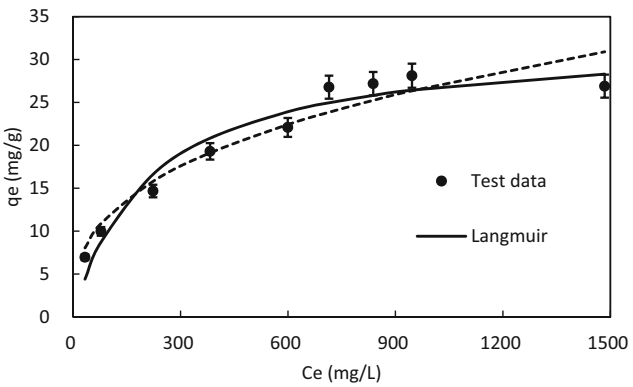

Fig. 9 Isotherm of nitrate adsorption onto Fe-CC

Table 4 Isotherm parameters of nitrate adsorption by Fe-CC

Isotherm	Parameters				
	q_e (mg/g)	K (L/mg)	K_f ($mg^{(1-n)}L^n/g$)	n (mg/g)	R^2
Langmuir	32.33	0.005	–	–	0.947
Freundlich	–	–	2.332	0.354	0.932

To determine the maximum adsorption of Fe-CC for nitrate, the modified biochar was contacted with varying initial concentrations (50–1500 ppm) of nitrate. The pattern of adsorption process is shown in Fig. 9. The adsorption capacity increased with the increasing initial concentration. Saturation started to establish when the equilibrium concentration was about 800 ppm. Langmuir and Freundlich models were applied to evaluate the experiment data and the fitting results are showed in Table 4. The best fitted model was Langmuir model whose correlation coefficient was 0.947, while the coefficient of Freundlich model was 0.932. According to the Langmuir model, maximum sorption capacity of Fe-CC to nitrate was 32.33 mg/g. This result indicates that the nitrate removal belonged to monolayer sorption (Xu et al. 2017).

Adsorption mechanism

Compared with pristine biochar, Fe-CC had a new crystal of Fe_2O_3. This was attributed to the $FeCl_3$ modification, which can be probably described as:

$$2FeCl_3 + 3H_2O \rightarrow^{\Delta} Fe_2O_3 + 6HCl$$

The difference in the XRD and FTIR analysis before and after adsorption of Fe-CC demonstrates that there was iron nitrate hydrate ($Fe(NO_3)_3{\cdot}9H_2O$) on the biochar surface after adsorption. The new substance was due to the following reaction in the adsorption, which led to the high adsorption capacity of Fe-CC onto nitrate.

$$Fe_2O_3 + 3H_2O \rightarrow 2Fe(OH)_3$$

$$Fe(OH)_3 + 3NO_3^- + 9H_2O \rightarrow Fe(NO_3)_3 \cdot 9H_2O + 3OH^-$$

The high surface charge indicates that Fe-CC was a perfect adsorbent to remove anions for electrostatic attraction. The multiple electrons of Fe led to the formation of coordination compound ($Fe(NO_3)_3{\cdot}9H_2O$). In addition, the considerably huge specific surface area in Table 5 indicates that surface adsorption played a role in the removal process.

Conclusion

In this work, different metal modifying agents were applied to treat the corncob. Metal modifying agents fixed metal ion on the biochars by forming metal oxide structures. This increased specific surface area and surface charge, leading to high adsorption capacity to anions. Metal possessing multilayer electrons with higher valence was a better modifying agent. Fe-CC with the highest zeta potential among these modified biochars showed the highest nitrate adsorption capacity. After modification, Fe_2O_3 was generated on the surface and nitrate anions were absorbed on Fe-CC. As a result, Fe_2O_3 was transformed to fix the nitrate by forming iron nitrate hydrate ($Fe(NO_3)_3{\cdot}9H_2O$). Based on results of the Langmuir model, the maximum capacity of Fe-CC to remove nitrate was 32.33 mg/g, which is much higher than those of previously reported adsorbents. For future application, Fe-CC ought to be studied to simultaneously remove nitrate, organic pollutants, and other natural common contaminants. Desorption and column studies will be conducted. And these adsorbents have potential application to soil remediation.

Table 5 The specific surface area and pore structure of different biochars

Biochars	BET surface area (m^2/g)	The micropore area (m^2/g)	The total pore volume (cm^3/g)	Micropore volume (cm^3/g)	The average pore size (nm)
CC	129.65				
Na-CC	37.18				
K-CC	82.90	68.98	0.05	0.04	48.96
Mg-CC	249.56	204.05	0.15	0.11	77.80
Zn-CC	230.86	184.48	0.12	0.09	32.05
Al-CC	148.37				
Fe-CC	155.08				
H + Mg-CC	301.81	252.94	0.18	0.13	48.54

Acknowledgments The authors thank the anonymous reviewers for their invaluable insight and helpful suggestions.

Funding information This work was partially supported by the Fundamental Research Funds for the Central Universities (No. 2042016kf0173) and the Wuhan Water Engineering & Technology Co. Ltd.

References

Calero J, Ontiveros-Ortega A, Aranda V (n.d.) Plaza I Humic acid adsorption and its role in colloidal-scale aggregation determined with the zeta potential, surface free energy and the extended-DLVO theory. Eur J Soil Sci

Choe E, Meer FVD, Rossiter D, Salm CVD, Kim KW (2010) An alternate method for Fourier transform infrared (FTIR) spectroscopic determination of soil nitrate using derivative analysis and sample treatments. Water Air Soil Pollut 206:129–137

Cosimo JID, DíEz VK, Xu M, Iglesia E, CR ApesteguíA (1998) Structure and surface and catalytic properties of Mg-Al basic oxides ☆. J Catal 178:499–510

Creamer AE, Gao B, Wang SS (2016) Carbon dioxide capture using various metal oxyhydroxide-biochar composites. Chem Eng J 283:826–832

De RG, Lahav M, Me VDB (2014) Pyridine coordination chemistry for molecular assemblies on surfaces. Acc Chem Res 47:3407

Ding Z, Hu X, Wan Y, Wang S, Gao B (2016) Removal of lead, copper, cadmium, zinc, and nickel from aqueous solutions by alkali-modified biochar: batch and column tests. J Ind Eng Chem 33:239–245

Du C, Cui CW, Qiu S, Shi SN, Li A, Ma F (2017) Nitrogen removal and microbial community shift in an aerobic denitrification reactor bioaugmented with a Pseudomonas strain for coal-based ethylene glycol industry wastewater treatment. Environ Sci Pollut Res 24: 11435–11445

Eeshwarasinghe D, Loganathan P, Kalaruban M, Sounthararajah DP, Kandasamy J, Vigneswaran S (2018) Removing polycyclic aromatic hydrocarbons from water using granular activated carbon: kinetic and equilibrium adsorption studies. Environ Sci Pollut Res 25: 13511–13524

Gao F, Xue YW, Deng PY, Cheng XR, Yang K (2015) Removal of aqueous ammonium by biochars derived from agricultural residuals at different pyrolysis temperatures. Chem Speciat Bioavailab 27:92–97

Hu X, Xue Y, Long L, Zhang K (2018a) Characteristics and batch experiments of acid- and alkali-modified corncob biomass for nitrate removal from aqueous solution. Environ Sci Pollut Res:1–9

Hu XL, Xue YW, Liu LN, Zeng YF, Long L (2018b) Preparation and characterization of Na2S-modified biochar for nickel removal. Environ Sci Pollut Res 25:9887–9895

Jung KW, Lee S, Lee YJ (2017) Synthesis of novel magnesium ferrite (MgFe2O4)/biochar magnetic composites and its adsorption behavior for phosphate in aqueous solutions. Bioresour Technol 245:751–759

Kang J, Duan X, Wang C, Sun H, Tan X, Tade MO, Wang S (2018) Nitrogen-doped bamboo-like carbon nanotubes with Ni encapsulation for persulfate activation to remove emerging contaminants with excellent catalytic stability. Chem Eng J 332:398–408

Liu G, Zhou Y, Liu Z, Zhang J, Tang B, Yang S, Sun C (2016a) Efficient nitrate removal using micro-electrolysis with zero valent iron/activated carbon nanocomposite. J Chem Technol Biotechnol 91: 2942–2949

Liu Z, Xue Y, Gao F, Cheng X, Yang K (2016b) Removal of ammonium from aqueous solutions using alkali-modified biochars. Chem Speciat Bioavailab 28:26–32

Long L, Xue Y, Zeng Y, Yang K, Lin C (2017) Synthesis, characterization and mechanism analysis of modified crayfish shell biochar possessed ZnO nanoparticles to remove trichloroacetic acid. J Clean Prod 166:1244–1252

Lu X, Jiang J, Sun K, Zhu G, Lin G (2016) Enhancement of Pb2+ removal by activating carbon spheres/activated carbon composite material with H2O vapor. Colloids Surf A Physicochem Eng Asp 506:637–645

Patwardhan SV, Emami FS, Berry RJ, Jones SE, Naik RR, Deschaume O, Heinz H, Perry CC (2012) Chemistry of aqueous silica nanoparticle surfaces and the mechanism of selective peptide adsorption. J Am Chem Soc 134:6244

Qiu Y, Moore S, Hurt R, Külaots I (2017) Influence of external heating rate on the structure and porosity of thermally exfoliated graphite oxide. Carbon 111:651

Sarkar B, Mandal S, Tsang YF, Kumar P, Kim KH, Yong SO (2018) Designer carbon nanotubes for contaminant removal in water and wastewater: a critical review. Sci Total Environ 612:561–581

Sembiring S, Simanjuntak W, Manurung P, Asmi D, Low IM (2014) Synthesis and characterisation of gel-derived mullite precursors from rice husk silica. Ceram Int 40:7067–7072

Sofer Z, Jankovský O, Šimek P, Sedmidubský D, Šturala J, Kosina J, Mikšová R, Macková A, Mikulics M, Pumera M (2015) Insight into the mechanism of the thermal reduction of graphite oxide: deuterium-labeled graphite oxide is the key. ACS Nano 9:5478–5485

Tanboonchuy V, Hsu JC, Grisdanurak N, Liao CH (2011) Impact of selected solution factors on arsenate and arsenite removal by nanoiron particles. Environ Sci Pollut Res 18:857–864

Tytak A, Oleszczuk P, Dobrowolski R (2015) Sorption and desorption of Cr(VI) ions from water by biochars in different environmental conditions. Environ Sci Pollut Res 22:5985–5994

Villegas-Guzman P, Hofer F, Silva-Agredo J, Torres-Palma RA (2017) Role of sulfate, chloride, and nitrate anions on the degradation of fluoroquinolone antibiotics by photoelectro-Fenton. Environ Sci Pollut Res 24:28175–28189

Wan S, Wang S, Li Y, Gao B (2017) Functionalizing biochar with Mg–Al and Mg–Fe layered double hydroxides for removal of phosphate from aqueous solutions. J Ind Eng Chem 47:246–253

Wang SS, Gao B, Zimmerman AR, Li YC, Ma L, Harris WG, Migliaccio KW (2015) Removal of arsenic by magnetic biochar prepared from pinewood and natural hematite. Bioresour Technol 175:391–395

Wang B, S-y L, F-y L, Z-p F (2016) Removal of nitrate from constructed wetland in winter in high-latitude areas with modified hydrophyte biochars. Korean J Chem Eng 34:717–722

Wang S, Li X, Liu Y, Zhang C, Tan X, Zeng G, Song B, Jiang L (2017) Nitrogen-containing amino compounds functionalized graphene oxide: synthesis, characterization and application for the removal of pollutants from wastewater: a review. J Hazard Mater 342:177

Xiao Y, Xue Y, Gao F, Mosa A (2017) Sorption of heavy metal ions onto crayfish shell biochar: effect of pyrolysis temperature, pH and ionic strength. J Taiwan Inst Chem Eng

Xu X, Hu X, Ding Z, Chen Y, Gao B (2017) Waste-art-paper biochar as an effective sorbent for recovery of aqueous Pb(II) into value-added PbO nanoparticles. Chem Eng J 308:863–871

Xue YW, Gao B, Yao Y, Inyang M, Zhang M, Zimmerman AR, Ro KS (2012) Hydrogen peroxide modification enhances the ability of biochar (hydrochar) produced from hydrothermal carbonization of peanut hull to remove aqueous heavy metals: batch and column tests. Chem Eng J 200:673–680

Xue L, Gao B, Wan Y, Fang J, Wang S, Li Y, Muñoz-Carpena R, Yang L (2016) High efficiency and selectivity of MgFe-LDH modified wheat-straw biochar in the removal of nitrate from aqueous solutions. J Taiwan Inst Chem Eng 63:312–317

Yao Y, Gao B, Inyang M, Zimmerman AR, Cao XD, Pullammanappallil P, Yang LY (2011) Biochar derived from anaerobically digested sugar beet tailings: characterization and phosphate removal potential. Bioresour Technol 102:6273–6278

Yao Y, Gao B, Zhang M, Inyang M, Zimmerman AR (2012) Effect of biochar amendment on sorption and leaching of nitrate, ammonium, and phosphate in a sandy soil. Chemosphere 89:1467–1471

Yu F, Zhou Y, Gao B, Qiao H, Li Y, Wang E, Pang L, Bao C (2016) Effective removal of ionic liquid using modified biochar and its biological effects. J Taiwan Inst Chem Eng 67:318–324

Zhang M, Gao B, Yao Y, Xue YW, Inyang M (2012) Synthesis of porous MgO-biochar nanocomposites for removal of phosphate and nitrate from aqueous solutions. Chem Eng J 210:26–32

Zhang M, Gao B, Yao Y, Inyang M (2013) Phosphate removal ability of biochar/MgAl-LDH ultra-fine composites prepared by liquid-phase deposition. Chemosphere 92:1042–1047

Zhang F, Wang X, Xionghui J, Ma L (2016) Efficient arsenate removal by magnetite-modified water hyacinth biochar. Environ Pollut 216: 575–583